CEAS Aeronautical Journal
https://doi.org/10.1007/s13272-026-00955-1

ORIGINAL PAPER

Towards laser-doppler-vibrometry with UAVs - the effect of wind disturbances on the position of a mirror attached to a drone

Robin Zimmermann[1] · Umut Durak[1] · Mohamed A. A. Ismail[1,2]

Received: 4 March 2025 / Revised: 19 December 2025 / Accepted: 3 February 2026

Abstract

Recently there has been an interest in using laser Doppler vibrometers (LDVs) in combination with multirotor drones for structural health monitoring (SHM) of large structures like bridges or wind turbines. In order to easily position the measurement beam of the LDV on any point of the structure, a new measurement system is being developed for redirecting the beam using a mirror carried by a drone. A tracking system will have to be designed that will keep the laser beam centered on the mirror. However, the wind's influence on the movement of the mirror is unknown and consequently the requirements for the tracking system are unclear. In this work, tests with a 3D anemometer and DJI's Matrice 300 are carried out outdoors to determine the drone's dynamic response to wind fluctuations. The drone's angular movement correlates well with the wind speed, indicating the validity of the tests. The findings give a clear overview of the disturbance rejection performance of this commercially available drone operating under realistic wind conditions, using high-resolution wind measurement data and can inform the development of requirements for applications involving a directed beam aimed at a drone.

Keywords UAV · Laser-doppler-vibrometer · Wind · Dynamic · Displacement

List of Symbols

$\ddot{x}$	Acceleration m/s^2
ϕ	Bank rad
S	Cross sectional area m^2
ρ	Air density kg/m^3
C_D	Drag coefficient
D	Drag force N
$\mathbf{f_D}$	Translational drag force N
g	Gravitational acceleration m/s^2
Ψ	Heading rad
m	Mass kg
θ	Pitch rad
q	Unit quaternion
$\mathbf{r_{center}}$	Mirror displacement from drone's takeoff point m
$\mathbf{r_{drone}}$	Drone displacement from drone's takeoff point m
$\mathbf{r_{mirror}}$	Mirror offset from drone's center of mass m
R	Rotation matrix
R_{IB}	Rotation matrix (body to inertial frame)
$\mathbf{t_B}$	Thrust vector N
v_a	True airspeed m/s

Abbreviations

FRD	Forward-Right-Down
IMU	Inertial measurement unit
LDV	Laser Doppler vibrometer
NED	North-East-Down
OSDK	Onboard SDK
RTK	Real Time Kinematics
SHM	Structural health monitoring

These authors contributed equally to this work.

✉ Robin Zimmermann
robin.zimmermann@dlr.de

[1] Institute of Flight Systems, German Aerospace Center (DLR), Braunschweig 38108, Germany

[2] Interdisciplinary Research Center for Aviation and Space Exploration, Aerospace Department, King Fahd University of Petroleum & Minerals (KFUPM), Dhahran 31261, Saudi Arabia

Published online: 12 February 2026

1 Introduction

There are many use cases in which drones as a sensor platform are used for visual inspection and monitoring of civil engineering structures e.g. for the inspection of power lines [1] or damaged bridges [2]. Another use case is SHM through vibration measurements. This can be done by using visual sensors on the drone in combination with fiducial markers [3] or by post-processing the image data using machine learning techniques [4]. A fairly recent development is the use of laser sensors to measure vibrations in large engineering structures like wind turbines, bridges, historic buildings etc. Herrmann et al. are using a laser triangulation displacement sensor on a drone to measure the vibrations of a wind turbine. Not only the desired absolute movement of the wind turbine but also the relative movement of the drone itself with respect to the target structure is included in the measurement signal of the displacement sensor. It is determined by two MEMS angular rate sensors and an accelerometer and then filtered out of the signal from the displacement sensor [5]. Nasimi et al. developed a similar setup that they use for measuring the vibrations of a bridge. In addition to a laser rangefinder, they also installed a camera on the drone for tracking a fixed checkerboard pattern on the ground. This enables them to filter out the influence of the drone's movement on the laser sensor measurement [6–8]. LDVs use a laser to measure surface vibrations from a distance without contact. They also lend themselves to SHM [9]. However, their use in SHM for large structures is limited, as their signal quality depends on the measurement distance, the surface finish and most importantly also on the angle of incidence between the laser and the measured surface [10]. Today, LDVs are sold that are marketed with a measurement range exceeding 300 m [11]. This range would enable LDVs to be used for monitoring the vibrations of many larger engineering structures, if it were not for the influence of the angle of incidence on the strength of the LDV's returning signal. Therefore it would be desirable to have a mobile LDV, that can be re-positioned at will to keep this angle as small as possible. One way to achieve this, although very cumbersome, is to put the LDV on a lifter, similar to how it has been done by Esposito et al. [12]. An optimal solution would involve a robot or a drone that can direct the laser beam to any desired measurement point with a low angle of incidence. This has been done by Garg et al. who mounted an LDV on a drone in order to collect displacement measurements of a moving target structure [13, 14]. The downside of this approach are the regulations that need to be followed when a drone powerful enough to carry an LDV is to be operated inside a city or any populated area for that matter [15]. Current LDVs weigh multiple kilograms and there are still technical challenges to be overcome for their miniaturization [16]. To solve this problem, a novel measurement setup is being researched, in which the LDV's laser is reflected by a mirror attached to a drone [17]. This way, the LDV's measurement beam can easily be maintained at a perpendicular angle of incidence on the surface of the structure under investigation without the need to physically relocate the LDV for each measurement point. Compared to the method where the LDV is put on a lifter, this greatly reduces the time needed for a measurement campaign. Additionally, because the drone's payload consists only of a mirror and not the whole LDV, it can be small enough to be flown almost anywhere without restrictions. Several papers have been published to show the feasibility of this new measurement setup. Schewe et al. investigated how different disturbances affect the vibration measurement [18]. Measurements from an LDV and a Differential-Laser-Doppler-Vibrometer were compared with disturbances resulting from turbulence in the optical path and from movements of the gimbal holding the mirror that is reflecting the measurement beam [19]. They also analyzed the influence of the drone's movement on the measurement signal [20]. Halkon and Rothberg subjected the LDV itself and a beam steering mirror to vibrations and subsequently corrected for these disturbances in the measurement signal using accelerometer data [21]. For an in-depth overview of the current state of the art regarding the use of unmanned aerial systems and LDVs to measure vibrations in large structures, the reader is advised to refer to the work of Rembe et al. [22]. For the complete measurement setup to work, not only the effects of disturbances on the LDV's measurement signal need to be investigated but also the problem of aligning the laser with the flying mirror needs to be solved, so that it can be held stable and at a fixed angle on the measurement surface. As can be seen in [20], to date alignment has been performed manually by placing the LDV on a simple tripod, setting the mirror on the drone to a fixed angle and then flying it into the optical path of the LDV's laser. The alignment achieved by this method is temporary. Any wind-induced external force acting on the drone will displace it and break the optical connection. The effect wind has on multirotor aircrafts is still an active field of study. Wei et al. [23] presents a systematic experimental study in which wind effects on a hovering multirotor are directly measured using a high-precision anemometer and incorporated into a system-identification framework, yielding wind-dependent state-space models that significantly improve prediction accuracy under outdoor conditions. By treating wind as an explicit input, the authors demonstrate that including wind correction terms reduces acceleration prediction errors by approximately 15% on average, and that increasing wind speed alters the damping and natural frequency of the vehicle's longitudinal dynamics. Juhasz et al. [24] similarly investigate wind and turbulence effects on a quadrotor using system identification from flight data, modeling atmospheric disturbances as control-equivalent turbulence inputs that reproduce observed motion degradation. Together, these works establish complementary identification-based frameworks for quantifying and modeling wind disturbances acting on multicopter UAVs during hover and low-speed flight. The goal for future work is an active alignment of the laser beam, where the LDV is placed on a motorized pan-tilt unit so that it can follow any movements of the mirror caused by wind fluctuations or similar disturbances. Because the drone's movement in response to wind fluctuations is unknown, this work will focus on determining the drone's dynamic response to wind speed and direction changes and how the angular rotation of the drone is affecting the mirror's movement. In future work, the findings from this analysis will serve as the basis for the requirements of the active tracking system for the LDV. In the first section a short overview over the complete system concept is given, then the method for realizing the wind test and its setup is defined. Finally the test results are shown and discussed in order to derive some recommendations for the tracking and the mirror-gimbal system.

2 General system description

To put the tests evaluating the drone's ability to handle wind disturbances into context, the measurement system concept to be realized in future work is shown in Fig. 1. Here, the LDV is put on a pan-tilt unit that receives commands from a control unit on the ground. The latter calculates the commands based on pose information from the drone and visual information from a camera integrated in the LDV. The target is the mirror on the drone. It is gimballed, enabling the drone to redirect the LDVs beam to a desired point on the measured object. Clearly a change in the mirrors position relative to the measured point would also cause a change in the laser beam's incidence angle which affects the measurement quality. Gaining an understanding of the maximum displacement of the mirror due to wind disturbances is therefore also the basis for future work looking into the optimal positioning of the components of the system relative to each other.

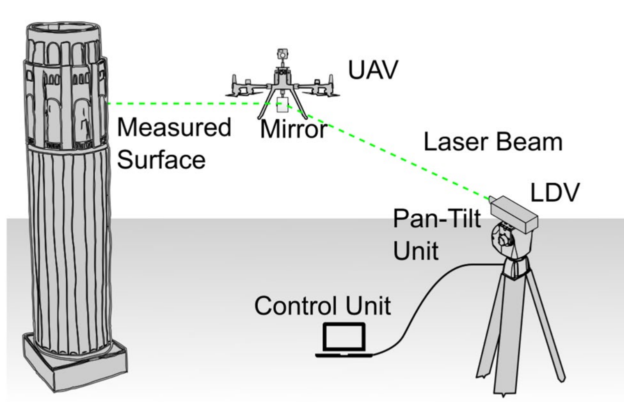

Fig. 1 Measurement system setup concept

3 Method

The utilized drone is the Matrice 300 made by DJI. Its hovering movement in varying wind is tested using a 3D anemometer with the drone flying besides it. It is flown at roughly 3 m, on the same height level of the anemometer. Several meters distance are maintained, so that the draft from the drone's propellers does not influence the measurement. Because the local wind conditions cannot be predicted reliably by looking at the weather report, the test had to be carried out two times for speeds over 10 m/s to be observed in situ. This is close to the drone's specified wind resistance for starting and landing at 12 m/s. During the wind tests a Real Time Kinematics (RTK) base station is employed to provide the drone with global navigation satellite system (GNSS) correction data. This way, the position measurement accuracy is raised to below 2 cm. Besides the RTK corrected position data, the drone's inertial measurement unit (IMU) sensor data is recorded. The drone is flown in 'P-mode' which is the manufacturer's term for the positioning hold mode. Herein the drone utilizes its GNSS module and vision system to stabilize its position [25]. During the measurement periods, there is no pilot intervention so that the drone's ability to hold its position is dependent solely on the manufacturers implementation of the positioning hold mode.

4 Wind-test setup

The setup to measure the drone's response to wind fluctuations is shown in Fig. 2. Two tests were conducted. One in Hillerse, Germany at Latitude 52.419 and Longitude 10.435 on 10th July 2024 between 11:17-11:46 CEST and another one in Hecklingen, Germany at Latitude 51.857 and Longitude 11.418 on 24th July 2024 between 14:09-15:00 CEST. The test in Hecklingen, which will be the main focus of this work, was conducted in even terrain where the next obstacle was a 13 m high building at 50 m distance in north direction, not in line with the prevailing wind direction. The anemometer was set up for its vertical axis to be perpendicular to the ground but not to point in a specific direction. Its horizontal orientation was later determined by comparing its wind direction 10 min average with the 10 min averages of the

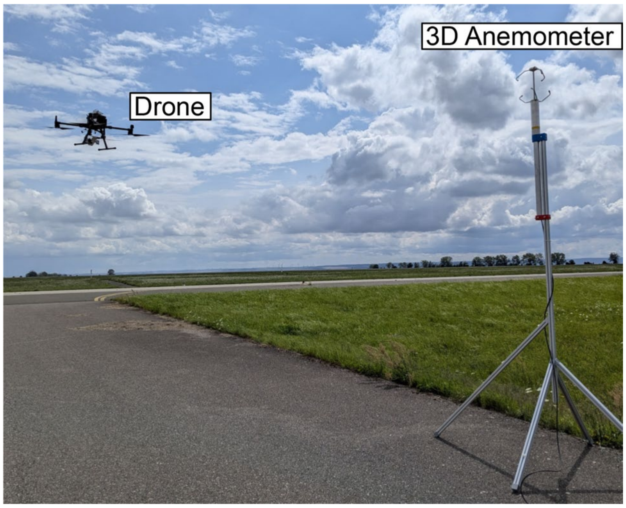

Fig. 2 Windtest Measurement Setup

Table 1 Wind Sensor Specifications

Model	4.383x - thies clima
Measurement range	0.01 - 85 m/s
Accuracy	±0,1 m/s + 1 % of the measurement value rms
Resolution	0,01 m/s
Sampling rate	252 Hz

Table 2 Drone and RTK reference station specifications

Model	DJI Matrice 300
Weight with batteries	6.3 kg
Max payload	2.7 kg
Max wind resistance (while starting/landing)	15 m/s (12 m/s)
Hovering accuracy (RTK enabled, windless or breezy)	Vertical: ±0.1 m Horizontal: ±0.1 m
Model	DJI D-RTK 2
Positioning accuracy single point	Horizontal: 1.5 m RMS Vertical: 3 m RMS
Positioning accuracy RTK	Horizontal: 1 cm + 1 ppm RMS Vertical: 2 cm + 1 ppm RMS
Positioning update rate	5 Hz

two local weather stations, which were located at opposite sides of the test location at distances of 1.3 and 1.2 kilometers respectively. The specifications of the anemometer and the drone are shown in table 1 and table 2 respectively. To record the drone's GNSS and internal IMU data, DJI's Onboard SDK (OSDK) [26] as the software interface is used. It is running on a RaspberryPi 4 that is mounted to the drone. This way, the drone's pose angles are recorded by the onboard computer at 400 Hz. The measurements are synchronized after the tests by comparing the timestamps given by the drone's GNSS module and the timestamps given to the anemometer data by the recording laptop.

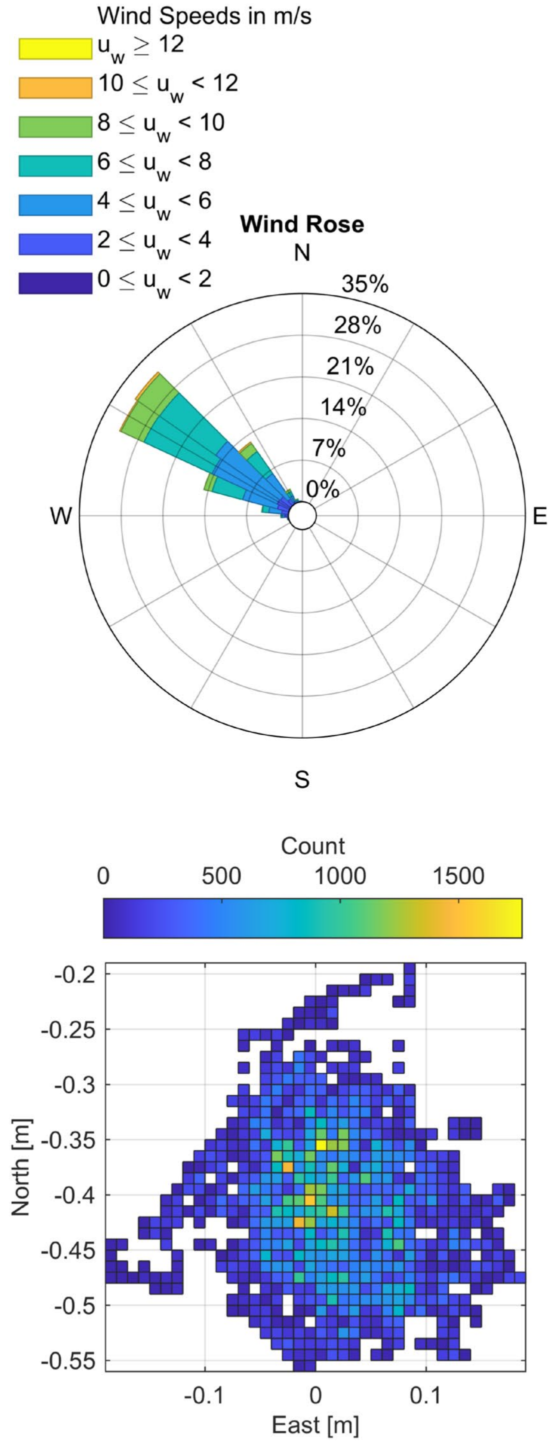

Fig. 3 Wind data visualized as a wind rose and drone's displacement during test visualized as a 2D-histogram

5 Results

The maximum wind speed magnitude was 6.1 m/s during the first test in Hillerse and 12.8 m/s during the second test in Hecklingen. Figure 3 is showing part of the results taken during the second test in windier conditions. There were no control inputs given for 481 s, during which the drone is operated in its default ’P-mode’, therefore stabilizing its position. The figure shows the horizontal movement of the drone in the earth-fixed North-East-Down(NED) coordinate frame given by the RTK corrected GNSS data. The maximum displacement of the drone is particularly relevant, because of the influence it has has on the incidence angle of the measurement laser on the target measuring point. Using the convex hull of the data for computational efficiency, the maximum distance between any two points during this time was determined to be 0.392 m. The maximum displacement in the horizontal plane is 0.354 m and with respect to the vertical axis it is 0.155 m. The data in Fig. 4 includes the same 481 s time frame up until second 832. In the upper plot the wind speed measured by the anemometer as well as the pitch angle and roll angle multiplied by -1 of the drone recorded by the internal IMU can be seen. The signals are smoothed using a moving average with a sliding window of 800 samples for the drone attitude data and 500 samples for the wind data in order to depict their progression more clearly. The wind speed signal shown includes the highest wind-speeds of 12.8 m/s measured during all testing, although the maximum speed peaks are dampened due to the aforementioned smoothing of the data. The horizontal wind direction angle is shown in Fig. 4. A strong correlation between the drone’s pitch angle and the wind speed can be observed in the first part of the plot until 832 s at which point the heading of the drone was changed by approximately 73 degrees. The Pearson correlation coefficient of 0.94 that is reached after optimizing the time delay between the two signals by means of cross-correlation also confirms this. The roll angle shows significantly smaller magnitudes than the pitch angle in the first part of the signal and seems to correlate with the change in wind direction. After the heading change at the 832 s mark the rotations about the roll-axis increase in magnitude while the pitch angles decrease. During the stationary parts the yaw angle changes shown in the lower graph are almost negligible. The time delay between the two signals is possibly caused by multiple effects which are the distance between the anemometer and the drone that is likely overcome quicker at higher wind speeds, clock drift of the Laptops internal clock that was last synchronized through the Network Time Protocol five hours before the test and the drone’s delayed response to the wind disturbance which is also dependent on its inertia.

Figure 5 is zoomed in on the time axis to the time interval containing the highest measured drone speed recorded during the two tests. The velocity signals here show the velocity of the point fixed to the geometric center of the mirror on the drone. The mirror’s eccentric position on the front of the drone means it will move relative to the earth-fixed NED

Fig. 4 Data showing correlation between wind and pitch, roll and yaw of drone

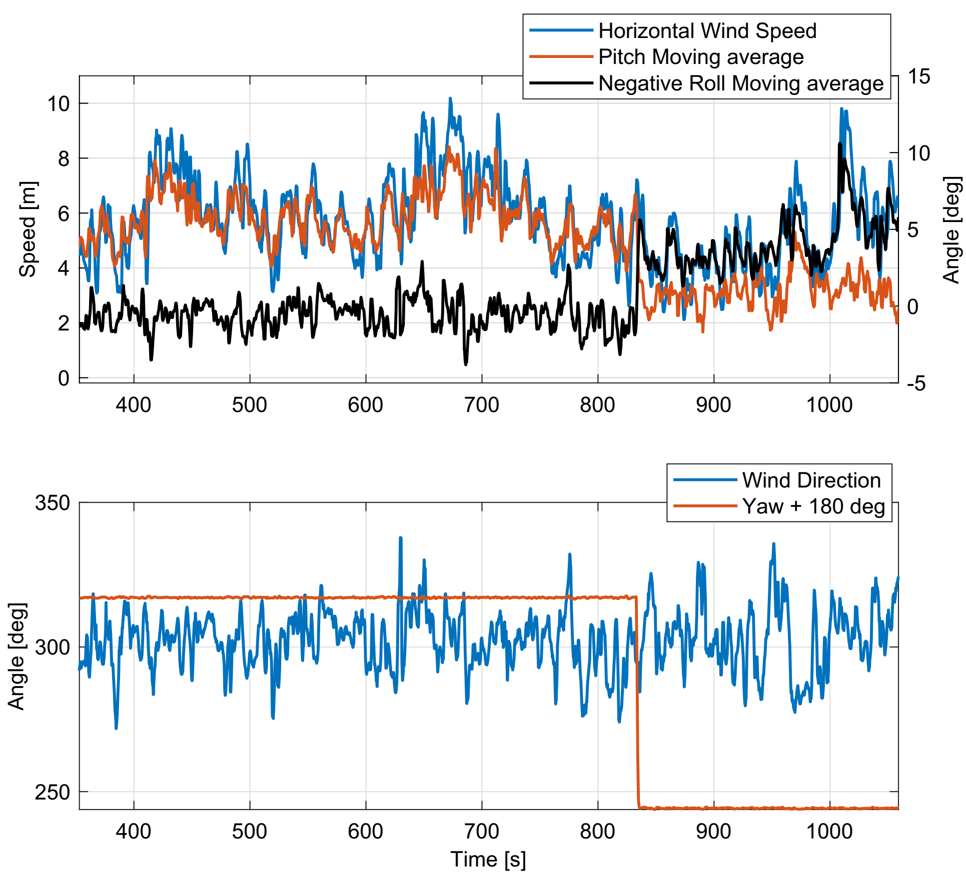

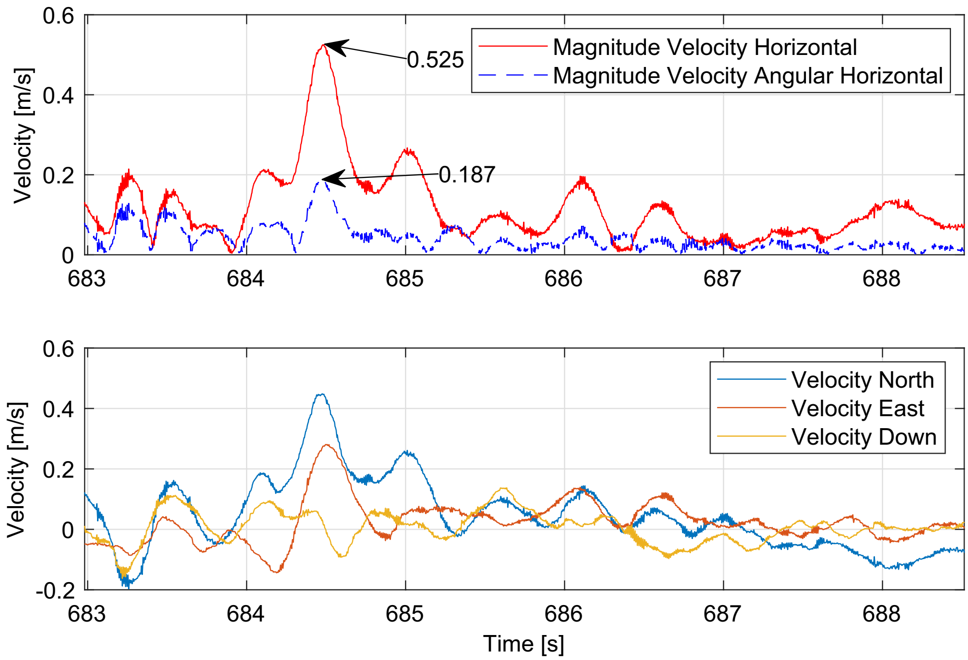

Fig. 5 Velocity of the mirror's center in the NED coordinate frame

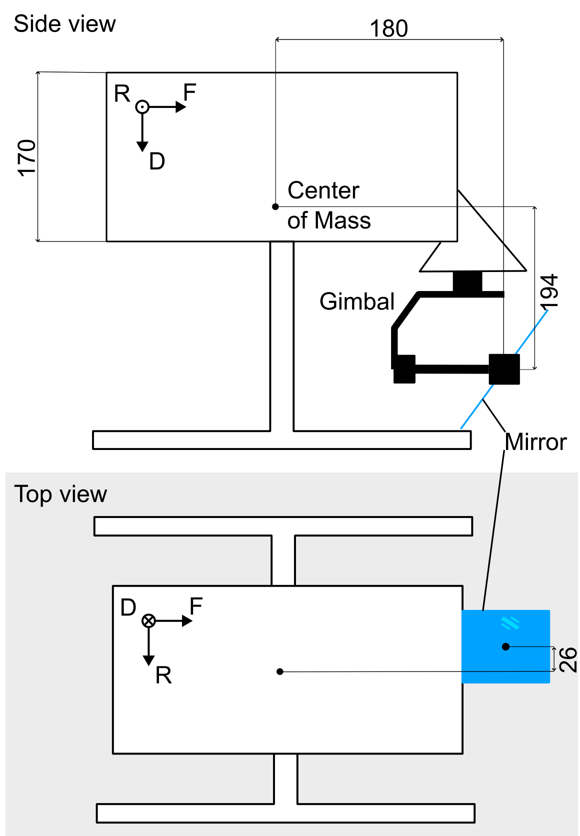

Fig. 6 Location of the drone's center of mass in mm

reference frame. The center of mass is estimated roughly by balancing the drone. Its location is shown in Fig. 6. The drone's angular pose is provided by the OSDK in quaternions. They are converted to Euler angles in the Aerospace Sequence convention $\Psi \rightarrow \theta \rightarrow \phi$ (heading, pitch, bank) from the ground frame NED to the body frame Forward-Right-Down (FRD) using

$$
\begin{aligned}
tan(\psi) &= \frac{m_{12}}{m_{11}} \\
sin(\theta) &= -m_{13} \\
tan(\phi) &= \frac{m_{23}}{m_{33}}
\end{aligned}
\tag{1}
$$

with

$$
\begin{aligned}
m_{11} &= 2q_0^2 + 2q_1^2 - 1 \\
m_{12} &= 2q_1q_2 + 2q_0q_3 \\
m_{13} &= 2q_1q_3 - 2q_0q_2 \\
m_{23} &= 2q_2q_3 + 2q_0q_1 \\
m_{33} &= 2q_0^2 + 2q_3^2 - 1
\end{aligned}
\tag{2}
$$

as the converting equation, adapted from [26] and [27]. $q = q_0 + q_1 + q_2 + q_3$ is the unit quaternion. To transform the body-fixed frame coordinates of the drone to NED Coordinates, the well known rotation matrix

$$
R = \begin{bmatrix} c\theta c\psi & -c\phi s\psi + s\phi s\theta c\psi & s\phi s\psi + c\phi s\theta c\psi \\ c\theta s\psi & c\phi c\psi + s\phi s\theta s\psi & -s\phi c\psi + c\phi s\theta s\psi \\ -s\theta & s\phi c\theta & c\phi c\theta \end{bmatrix}
\tag{3}
$$

is used where $c\varphi$ is $\cos\varphi$ and $s\varphi$ is $\sin\varphi$. The displacement of the mirror's center in the NED coordinate frame is given by

$$
\mathbf{r}_{\mathbf{center}}^{\mathbf{NED}} = \mathbf{r}_{\mathbf{drone}}^{\mathbf{NED}} + R\mathbf{r}_{\mathbf{mirror}}^{\mathbf{FRD}}.
\tag{4}
$$

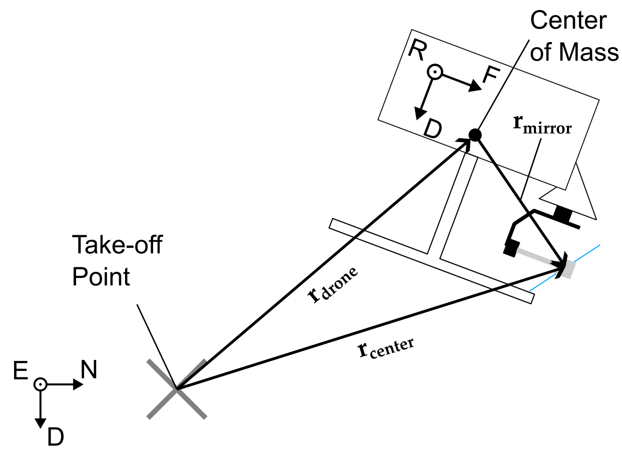

Fig. 7 Visualization of the drone's displacement vector

Table 3 Measurement signal's standard deviation and mean while drone is static on the ground

	Standard deviation	Mean
Yaw	0.0302 deg	N/A
Pitch	0.0122 deg	N/A
Roll	0.0091 deg	N/A
Velocity total Horizontal	1.4 mm/s	2.6 mm/s
Angular velocity Horizontal	1.4 mm/s	0.7 mm/s
Velocity North	1.5 mm/s	−1.9 mm/s
Velocity East	1.0 mm/s	−1.2 mm/s
Velocity Down	0.7 mm/s	0.2 mm/s

$\mathbf{r}^{\mathbf{NED}}_{\mathbf{drone}}$ Is the distance between the drone's starting point and the current position in the NED frame. $\mathbf{r}^{\mathbf{FRD}}_{\mathbf{mirror}}$ is the distance between the drone's center of mass and the geometrical center of the mirror in the FRD frame and $\mathbf{r}^{\mathbf{NED}}_{\mathbf{center}}$ is the distance between the drone's take-off point and the mirror's center. This is visualized in Fig. 7. To calculate the velocity of the mirrors center, the drone's velocity fusion signal is recorded at 200 Hz and the differentiated angular displacement $\dot{\mathrm{r}}^{NED}_{mirror}$ of the mirror is added. To reduce the high-frequency components of the signal, it is also smoothed using a moving average filter with just 10 samples. Using the euclidean norm

$$||[\dot{r}_N, \dot{r}_E]^\top||_2 \tag{5}$$

on the first two components of the vector $\dot{\mathrm{r}}^{NED}_{mirror}$, the horizontal velocity magnitude resulting only from the angular motion of the drone can be determined. The total horizontal velocity magnitude resulting from both angular and translational motion can be computed the same way using the vector $\dot{\mathrm{r}}^{NED}_{center}$. The upper graph in Fig. 5 clearly shows, that the contribution from the angular velocity is significant, making up $(0.187/0.525) \cdot 100\,\% = 35.61\,\%$ of the velocity's magnitude in the horizontal plane. To determine the influence of sensor noise and zero offset on the results, the standard deviations and where applicable also the mean values of the measured signals supplied by the drone's flight control system are given in Table 3. They were calculated from a part of the measurement signal during which the drone was static on the ground for 45.5 s with inactive motors.

6 Discussion

The tests were conducted outside in order to reproduce the operating conditions of the measurement system concept as closely as possible with GNSS support and highly variable wind speeds. But because of the nature of the test there are few controlled parameters. Consequently the measurement results offer a more qualitative than quantitative informative value. They will be utilized to assess the potential challenges in the development of the mirror tracking system and to determine the requirements for it. The currently used gimbaled mirror on the drone is 7.5 cm wide and 14 cm high. At the maximal horizontal mirror velocity it would mean that in ideal conditions, where the mirror is pointing directly towards the LDV on the pan-tilt Unit, the LDV would miss the mirror within $7.5\,\mathrm{cm}/(2 \cdot 52.5\,\mathrm{cm/s}) = 71.4\,\mathrm{ms}$ if no corrective action was taken. This reaction time is still achievable for the tracking system but the margin for error quickly diminishes when considering that the projected area of the mirror becomes smaller when it is tilted relative to the LDV in order to reflect its beam. This is without considering any inaccuracies resulting from the angular resolution of the pan-tilt unit or the camera used for the tracking. The horizontal and vertical displacement of the drone around its hovering point should not cause any issues when measuring far away surfaces. In dense cities however where the drone would need to fly closer to buildings it could already have an impact on the LDV's measurement, causing the measurement laser to not hit the surface close to perpendicular anymore and therefore picking up more in-plane vibrations in the signal. Trying to optimize for the stability around the hover point however it should be remembered that the translational drag force D

$$D = -\frac{1}{2}\rho v_a^2 S C_D \tag{6}$$

depends on the square of the true airspeed v_a. It is also proportional to the cross sectional area *S*, to the air density ρ and to the drag coefficient C_D. Simplified, the linear motion of quadcopters is usually described as follows,

$$m\ddot{\mathrm{x}} = \begin{bmatrix} 0 \\ 0 \\ mg \end{bmatrix} + R_{IB}\mathbf{t_B} + \mathbf{f_D} \quad (7)$$

where *m* is the mass of the drone, $\ddot{\mathrm{x}}$ is its acceleration, R_{IB} is the rotation matrix to transform the thrust vector $\mathbf{t_B}$ from the body-fixed frame to the inertial frame and $\mathbf{f_D}$ is the aerodynamic force. The aerodynamic force depends on multiple factors such as the aircraft's orientation relative to the oncoming airflow and the interaction of the propeller with it etc. These effects are neglected for the sake of clarity in this discussion. For a more in-depth discussion of the aerodynamic forces the reader is referred to [28]. To minimize the drones displacement around its hovering point would mean setting the left side of Eq. 7 to zero. However, because the drone's thrust vectors are always facing in the direction of the rotor's axes, it is obvious that it needs to angle itself in order to compensate for any drag forces acting in the horizontal plane. Therefore there is a trade-off to be made between the velocity of the mirror resulting from an attitude change of the drone and the velocity resulting from translational movement which mainly depends on the distance between the mirror and the center of mass. Additionally, because the mirror always has a minimum size that is determined by the tracking system's dynamics and it's angular resolution, the ratio between the mirrors surface area and the cross section of the rest of the drone is increasing as the drones carrying the mirror become smaller. The relative increase of the drag force to the total thrust resulting from this should be considered when designing the system with smaller drones as it will also increase the angular movement of the drone in response to disturbances.

7 Conclusion

Off-the-shelf drones are increasingly used as platforms for the development of measurement systems in which they are not the central focus of research. How much displacement from the commanded position the drone permits due to wind disturbance needs to be considered beforehand. This is especially true for use-cases where a focused beam is redirected by drone-carried hardware, as the drone's displacement can significantly impact the beam's alignment. To evaluate the influence of wind fluctuations on the ability to track a mirror on a drone, namely the Matrice 300 by DJI, tests are done measuring the wind speed and the drone's pose relative to the inertial frame. They take place in an open unobstructed area, using a 3D anemometer to measure the wind speed and an onboard computer to record the pose information provided by the drone's flight controller. The test shows a good correlation between the angular motion of the drone and the wind speed. For aiming a directed beam at the drone it is found that the mirrors motion due to it's eccentric position relative to the center of mass of the drone is not negligible. The translational displacement of the drone from the set position is also large enough to potentially have a significant impact on the incidence angle of the reflected beam on the target surface. To keep the tracking error as low as possible it is suggested that further research is carried out to optimize the stability of the mirror by placing it closer to the rotation axes of the drone or by optimizing the drone's control algorithms towards mirror stability.

Author Contributions All authors contributed to the discussion and conceptualization. R.Z. carried out the measurements, analyzed the data and wrote the manuscript. U.D. and M.A.A.I. contributed with supervision. All authors reviewed the manuscript.

Funding Open Access funding enabled and organized by Projekt DEAL. Funded by the Deutsche Forschungsgemeinschaft (DFG, German Research Foundation) Project ID: 496079937

Data availability Data sets generated during the current study are available from the corresponding author on reasonable request.

Declarations

Conflict of interest Umut Durak, co-author of this paper, is also an editor of this journal, but was not involved in the review process. All other authors have no Conflict of interest to declare that are relevant to the content of this article.

References

1. Jalil, B., Leone, G.R., Martinelli, M., Moroni, D., Pascali, M.A., Berton, A.: Fault Detection in Power Equipment via an Unmanned Aerial System Using Multi Modal Data. Sensors **19**(13), 3014 (2019). https://doi.org/10.3390/s19133014. (Number: 13 Publisher: Multidisciplinary Digital Publishing Institute. Accessed 2024-08-13)
2. Ellenberg, A., Kontsos, A., Moon, F., Bartoli, I.: Bridge related damage quantification using unmanned aerial vehicle imagery. Struct. Control. Health Monit. **23**(9), 1168–1179 (2016). https://doi.org/10.1002/stc.1831. (Accessed 2024-08-14)
3. Ribeiro, D., Santos, R., Cabral, R., Saramago, G., Montenegro, P., Carvalho, H., Correia, J., Calçada, R.: Non-contact structural displacement measurement using Unmanned Aerial Vehicles and

video-based systems. Mechanical Systems and Signal Processing 160, 107869 (2021) https://doi.org/10.1016/j.ymssp.2021.107869 . Accessed 2024-08-13

4. Ribeiro, D., Santos, R., Cabral, R., Calçada, R.: Remote Inspection and Monitoring of Civil Engineering Structures Based on Unmanned Aerial Vehicles. In: Chastre, C., Neves, J., Ribeiro, D., Neves, M.G., Faria, P. (eds.) Advances on Testing and Experimentation in Civil Engineering: Materials, Structures And Buildings, pp. 123–144. Springer, Cham (2023). https://doi.org/10.1007/978-3-031-23888-8_6 Accessed 2024-08-15
5. Herrmann, R., Moortgat-Pick, A., Marx, S.: Vibration Analysis of Structures using a Drone (UAV) based Mobile Sensing Platform. e-Journal of Nondestructive Testing **25**(01) (2020). Accessed 2024-05-29
6. Nasimi, R., Moreu, F., Nasimi, M., Wood, R.: Developing Enhanced Unmanned Aerial Vehicle Sensing System for Practical Bridge Inspections Using Field Experiments. Transp. Res. Rec. **2676**(6), 514–522 (2022). https://doi.org/10.1177/03611981221075618. (Publisher: SAGE Publications Inc., Accessed 2024-08-15)
7. Nasimi, R., Moreu, F.: A methodology for measuring the total displacements of structures using a laser–camera system. Computer-Aided Civil Infrastruct. Eng. **36**(4), 421–437 (2021). https://doi.org/10.1111/mice.12652. (Accessed 2024-08-14)
8. Nasimi, R., Moreu, F., Fricke, G.M.: Sensor Equipped UAS for Non-Contact Bridge Inspections: Field Application. Sensors **23**(1), 470 (2023). https://doi.org/10.3390/s23010470. (Number: 1 Publisher: Multidisciplinary Digital Publishing Institute. Accessed 2024-08-14)
9. Nassif, H.H., Gindy, M., Davis, J.: Comparison of laser Doppler vibrometer with contact sensors for monitoring bridge deflection and vibration. NDT & E Int. **38**(3), 213–218 (2005). https://doi.org/10.1016/j.ndteint.2004.06.012. (Accessed 2024-08-13)
10. Esposito, E., Castellini, P., Paone, N., Tomasini, E.P.: Laser Signal Dependence on Artworks Surface Characteristics: A Study of Frescoes and Icons Samples. In: Dickmann, K., Fotakis, C., Asmus, J.F. (eds.) Lasers in the Conservation of Artworks, pp. 327–332. Springer, Berlin, Heidelberg (2005). https://doi.org/10.1007/3-540-27176-7_40
11. VibroFlex modulares Vibrometer Messystem. https://www.polytec.com/de/vibrometrie/produkte/einpunkt-vibrometer/vibroflex Accessed 2024-08-16
12. Esposito, E.: RECENT PROGRESS IN DIAGNOSTICS OF CIVIL STRUCTURES BY LASER VIBROMETRY. e-Journal of Nondestructive Testing **9**(11) (2004). Accessed 2024-08-16
13. Garg, P., Nasimi, R., Ozdagli, A., Zhang, S., Mascarenas, D.D.L., Reda Taha, M., Moreu, F.: Measuring Transverse Displacements Using Unmanned Aerial Systems Laser Doppler Vibrometer (UAS-LDV): Development and Field Validation. Sensors 20(21), 6051 (2020)https://doi.org/10.3390/s20216051 . Number: 21 Publisher: Multidisciplinary Digital Publishing Institute. Accessed 2024-05-29
14. Garg, P., Moreu, F., Ozdagli, A., Taha, M.R., Mascareñas, D.: Noncontact Dynamic Displacement Measurement of Structures Using a Moving Laser Doppler Vibrometer. J. Bridg. Eng. **24**(9), 04019089 (2019). https://doi.org/10.1061/(ASCE)BE.1943-5592.0001472. (Publisher: American Society of Civil Engineers. Accessed 2024-08-16)
15. Durchführungsverordnung (EU) 2019/947 der Kommission vom 24. Mai 2019 über die Vorschriften und Verfahren für den Betrieb unbemannter Luftfahrzeuge (Text von Bedeutung für den EWR.). Legislative Body: MOVE, COM (2019). http://data.europa.eu/eli/reg_impl/2019/947/oj/deu Accessed 2024-08-17
16. Li, Y., Dieussaert, E., Baets, R.: Miniaturization of Laser Doppler Vibrometers—A Review. Sensors **22**(13), 4735 (2022). https://doi.org/10.3390/s22134735. (Number: 13 Publisher: Multidisciplinary Digital Publishing Institute. Accessed 2024-08-14)
17. Ismail, M.A.A.M.: Verfahren und Vorrichtung zum Messen Von Schwingungen Eines Objekts Unter Verwendung Einer Drohne. DE102018113244B3, (2019) https://patents.google.com/patent/DE102018113244B3/en?oq=DE102018113244B3 Accessed 2024-08-15
18. Schewe, M., Ismail, M.A.A., Rembe, C.: Towards airborne laser Doppler vibrometry for structural health monitoring of large and curved structures. Insight - Non-Destruct. Test. Condit. Monit. **63**(5), 280–282 (2021). https://doi.org/10.1784/insi.2021.63.5.280. (Accessed 2024-04-15)
19. Schewe, M., Ismail, M.A.A., Rembe, C.: Differentielle Laser-Doppler-Vibrometrie für luftgestützte Vibrationsmessungen mit Drohnen. tm - Technisches Messen 88(s1), 42–47 (2021) https://doi.org/10.1515/teme-2021-0071 . Publisher: Oldenbourg Wissenschaftsverlag. Accessed 2024-08-15
20. Schewe, M., Ismail, M.A.A., Zimmermann, R., Durak, U., Rembe, C.: Flyable Mirror: Airborne laser Doppler vibrometer for large engineering structures. J. Phys: Conf. Ser. **2698**(1), 012007 (2024). https://doi.org/10.1088/1742-6596/2698/1/012007. (Publisher: IOP Publishing. Accessed 2024-08-15)
21. Halkon, B., Rothberg, S.: Taking laser Doppler vibrometry off the tripod. In: 25th International Congress on Sound and Vibration 2018, ICSV 2018: Hiroshima Calling (2018)
22. Rembe, C., Halkon, B.J., Ismail, M.A.A.: Measuring Vibrations in Large Structures with LDVy and UAS: A Review and Outlook. Advanced Devices & Instrumentation, 0103 (2025) https://doi.org/10.34133/adi.0103 . Accessed 2025-08-20
23. Wei, P., Lin, X., Kong, Z.: System identification of wind effects on multirotor aircraft. Int. J. Intell. Robot. Appl. **6**(1), 104–118 (2022). https://doi.org/10.1007/s41315-021-00185-0. (Accessed 2025-12-19)
24. Juhasz, O., Lopez, M.J., Berrios, M.G., Berger, T., Tischler, M.B.: Turbulence modeling of a small quadrotor uas using system identification from flight data. In: American Helicopter Society 73rd Annual Forum, pp. 9–11
25. Matrice 300 RTK - User Manual v4.0 - DJI Pilot 2 (2023). https://www.dji.com/downloads/products/matrice-300?backup_page=index&target=us#doc Accessed 2025-12-01
26. DJI Developer. https://developer.dji.com/onboard-sdk/ Accessed 2024-08-21
27. Kuipers, J.B.: Quaternions and Rotation Sequences: a Primer with Applications to Orbits, Aerospace, and Virtual Reality. Princeton University Press, Princeton (1999)
28. MASSÉ, C., GOUGEON, O., NGUYEN, D.-T., SAUSSIÉ, D.: Modeling and Control of a Quadcopter Flying in a Wind Field: A Comparison Between LQR and Structured H_∞ Control Techniques. In: 2018 International Conference on Unmanned Aircraft Systems (ICUAS), pp. 1408–1417 (2018). https://doi.org/10.1109/ICUAS.2018.8453402